HHS Public Access

Author manuscript

Exp Dermatol. Author manuscript; available in PMC 2018 September 01.

Published in final edited form as:

Exp Dermatol. 2017 September ; 26(9): 792–797. doi:10.1111/exd.13294.

The parathyroid hormone family member TIP39 interacts with sarco/endoplasmic reticulum Ca^{2+}- ATPase activity by influencing calcium homeostasis

Emi Sato[1], **Michael R Williams**[1], **James A Sanford**[1], **George L Sen**[1,2], **Takekuni Nakama**[3], **Shinichi Imafuku**[4], and **Richard L Gallo**[1]

[1] Department of Dermatology, University of California San Diego, La Jolla, CA, 92093

[2] Department of Cellular and Molecular Medicine, University of California San Diego, La Jolla, CA, 92093

[3] Department of Dermatology, Kurume University, Kurume, Fukuoka, Japan

[4] Department of Dermatology, Fukuoka University, Fukuoka, Fukuoka, Japan

Abstract

Darier disease (DD) is a genetic skin disease that is associated with mutations in the *ATP2A2* gene encoding the type 2 sarco/endoplasmic reticulum Ca^{2+}-ATPase (SERCA2). Mutations of this gene result in alterations of calcium homeostasis, abnormal epidermal adhesion and dyskeratosis. Silencing of *ATP2A2* in monolayer cell culture of keratinocytes reduces desmoplakin expression at the borders of cells and impacts cell adhesion. Here, we report establishment of a three-dimensional (3D) epidermal model of DD, and use this model to evaluate peptide therapy with tuberoinfundibular peptide of 39 residues (TIP39) to normalize calcium transport. Gene silencing of *ATP2A2* in keratinocytes grown in a 3D model resulted in dyskeratosis, partial parakeratosis and suprabasal clefts that resembled the histological changes seen in skin biopsies from patients with DD. TIP39, a peptide recently identified as a regulator of keratinocyte calcium transport, , was then applied to this *ATP2A2* silenced 3D epidermal model. In normal keratinocytes, TIP39 increased $[Ca^{2+}]_i$ through the inositol trisphosphate (IP3) receptor pathway and stimulated differentiation. In monolayer *ATP2A2*-silenced keratinocytes, although TIP39 increased cytosolic calcium from the endoplasmic reticulum (ER), the response was incomplete compared with its control. TIP39 was observed to reduce intercellular clefts of the gene silenced epidermal model but did not significantly upregulate keratinocyte differentiation genes such as keratin10 and

Corresponding author: Richard L Gallo, Department of Dermatology, University of California San Diego, 9500 Gillman Dr.,#0869, La Jolla, California, 92093, USA. rgallo@vapop.ucsd.edu.

Author Contribution

E.S. designed and performed a majority of the experiments and wrote the manuscript. M.R.W., J.A.S. and G.L.S. assisted with the experiment of 3D cultured keratinocyte model, T.N. gave the sections and genetic information of Darier disease patients, S.I. reviewed the manuscript and gave pathohistological advice. R.L.G. supervised and designed experiments and wrote and prepared the manuscript. All authors reviewed and approved the final version of the manuscript.

Conflict of Interest

RLG is a consultant and has equity interest in Sente and MatriSys Inc.

Ethics Approval

This study was approved by the local institutional review boards (approval number: 16-3-18, approved on April 15 2016) and was conducted in compliance with the guidelines of good clinical practice and the principles of the Declaration of Helsinki.

filaggrin. These findings indicate that TIP39 is a modulator of ER calcium signaling and may be used as a potential strategy for improving aspects of DD.

Keywords

Darier disease; ATP2A2; TIP39; intracellular calcium response; skin barrier disruption

Introduction

Darier disease (DD), also known as Darier-White disease, Dyskeratosis follicularis and Keratiosis follicularis, is an autosomal dominantly inherited skin disorder in which desmosomal adhesion between keratinocytes is abnormal (1-3). A mutation of the *ATP2A2* gene encoding type 2 sarco/endoplasmic reticulum Ca^{2+}-ATPase (SERCA2) is the primary genetic cause of this disease (4). SERCA2 controls the transport of calcium ions from the cytosol into the lumen of the endoplasmic reticulum. This gene mutation causes alterations of Ca^{2+} homeostasis, then induces loss of epidermal adhesion and dyskeratosis (1, 2). Keratinocyte adhesion defects have been proposed to be due to the influence of SERCA2 on desmoplakin dynamics and intracellular adhesive strength through PKCα signaling (5), and DD keratinocytes have been shown to display biochemical and morphological hallmarks of constitutive endoplasmic reticulum (ER) stress with increased sensitivity to ER stressors (6). There are currently no validated curative treatments available for DD, with the majority of cases treated symptomatically. Lifestyle advice is very important and topical steroids, vitamin D3 and oral retinoids are often used for DD therapies. For secondary bacterial and fungal infection, antibiotics and/or antifungal agents have been orally or topically administered (7).

Tuberoinfundibular peptide of 39 residues (TIP39) is a member of the parathyroid hormone (PTH) ligand family, and an agonist of the PTH second receptor (PTH2R) which is known as a class b G protein-coupled receptor (GPCR) (8). Recently, we reported that TIP39 directly binds to PTH2R on the ER at low extracellular calcium conditions (9). TIP39 regulates intracellular calcium ($[Ca^{2+}]_i$) of keratinocytes via PLC-inositol trisphosphate (IP3) receptor pathway (9). Here, we have established a DD-like three-dimensional (3D) epidermal model by silencing *ATP2A2* mRNA in keratinocytes, and investigated the effects of TIP39 on calcium transport and epidermal structure in this model.

Materials and methods

Cells and reagents

Normal human epidermal keratinocytes (NHEK) were cultured as previously described (9). 3D *in vitro* skin constructs were prepared as described (10). TIP39 peptides (10μM; Bachem Americas, Torrance, CA) or control peptides (10 μM; GenScript, Piscataway, NJ) were added to keratinocyte growth media for 6days.

Isolation of total RNA and quantitative RT-PCR

Total RNA from cultured keratinocytes and 3D in vitro skin constructs was extracted, and cDNA was synthesized as previously described (9). TaqMan Gene Expression Assays (Thermo Fisher Scientific, Waltham, MA) were used to analyze expression of human ATP2A2 (assay ID: Hs00544877_m1), human KRT5 (assay ID: Hs00361185_m1), human KRT10 (assay ID: Hs01043114_g1), human FLG (assa y ID: Hs00856927_g1) and human DSP (assay ID: Hs00950591_m1) as described by the manufacturer's instructions. Human GAPDH (assay ID: Hs02758991_g1) was used as an internal control to validate RNA for each sample. Each mRNA expression was calculated as the relative expression to GAPDH, and all data are presented as fold change against each control (mean of non-stimulated cells).

siRNA transfection to NHEK

ATP2A2 and control siRNA were purchased from GE Dharmacon (Lafayette, CO). siRNA transfection was performed by manufacturer's instructions of Lipofectamine® RNAiMAX (Thermo Fisher Scientific). To silence ATP2A2 in a 3D skin construct, 300pmol siRNA were transfected to 2×10^6NHEK in $6cm^2$ culture dish. Cells were harvested at 18h after transfection, and used for production of the 3D skin construct as previously described (10).

Western blot

Protein isolation and transfer were performed as previously described (9). Anti-ATP2A2 (1μg/mL; Santa Cruz, Dallas, TX) and anti-GAPDH (1μg/mL; North Acton, MA) antibodies were used for protein detection. Six-hundred and eighty nanometer and 800 nm IR-Dye conjugated secondary antibodies (1:10000) and an Odyssey imager and quantification software (LI-COR Biosciences, Lincoln, NE) were used for two-color western blotting to analyse both proteins on the same blot.

Immunohistochemistry for paraffin-embedded sections

Immunohistochemistry staining (IHC) was performed as previously described (11). Paraffin skin sections of Darier disease were obtained from Kurume University (Kurume, Fukuoka, Japan). 4-μm paraffin sections were deparaffinized and rehydrated before heat-induced antigen retrieval was performed in 10mM citrate buffer (pH 6.0). Anti-E-cadherin (CST, MA) and Anti-PTH2R was a gift of Dr. Usdin (NIMH, Bethesda, MD). DAB staining was performed by Lab Vision™ UltraVision™ ONE Detection System: HRP Polymer/DAB Plus Chromogen (Thermo Fisher Scientific). Images were captured using a BX41 microscope (Olympus, Center Valley, PA).

Immunofluorescence staining of cultured cells

Cells were fixed in −20°C cold methanol for 10 minutes then blocked with PBS containing 5% donkey serum at room temperature for 30 minutes. Immunostaining was performed as previously reported (9). Anti-Desmoplakin I+II (Abcam, Cambridge, MA), secondary Alexa Fluor 488 or 594-conjugated antibodies (Thermo Fisher Scientific) were used at 1μg/mL. Cover slips were mounted using ProLong® Gold antifade Reagent with DAPI (Thermo Fisher Scientific). Images were captured using a BX41 microscope (Olympus).

Intracellular calcium image and measurements

Intracellular calcium measurement was performed as previously described (Sato et al., 2016). NHEK were seeded at 4×10^4/well (or 1×10^4/well for siRNA experiment) one day before experiments. For testing calcium reaction in the endoplasmic reticulum, we used calcium free balanced salt solution with 150μM EGTA. 10 or 25μM TIP39 peptide (Bachem), 5μM thapsigargin, 5 or 10μM ionomycin (Enzo Life Science) and 2 or 2.5 mM $CaCl_2$ were added as indicated in dye loading solution then Intracellular calcium was monitored at an emission of 516 nm with excitation of 494 nm using SpectraMax Gemini EM microplate Reader (Molecular Devices, Sunnyvale, CA). Fluo-4 signal changes (%) were defined as (F-F0) / F0 × 100. F was the target fluorescence signal intensity and F0 was the baseline calculated by averaging five time points just prior to the application of the stimulus. Intracellular calcium images were captured using a BX41 microscope (Olympus).

Statistical analysis—Data are expressed as means ± SEM. Differences between experimental groups within each experiment were analyzed using the unpaired Student t test and were considered significant at $p \leq 0.05$.

Results

TIP39 increased cytosolic calcium from the endoplasmic reticulum and might improve SERCA activity after supplementation of calcium

The endoplasmic reticulum (ER) is the main dynamic Ca^{2+} storage compartment of the cell (12-14). We previous reported that exogenous TIP39 colocalized with the ER 5 minutes after application, and increased $[Ca^{2+}]_i$ via $G\alpha_q$-PLC-IP3 pathway at low extracellular calcium conditions (9). Activated-PLC is known to hydrolyze phosphatidylinositol 4,5-bisphosphate ($PI(4,5)P_2$) to produce diacylglycerol (DAG) and IP3. DAG and the reduction of $PI(4,5)P_2$ levels directly contribute to activation of transient receptor potential cation (TRPC) channels, while IP3 triggers Ca^{2+} release from intracellular stores (15). Therefore, these complex interactions suggest TIP39 might increase cytosolic calcium not only from the ER store but also from the extracellular space. Thus, , we investigated the effects of TIP39 with the intent of determining the source of increased cytosolic $[Ca^{2+}]$. Figure 1a shows that TIP39 increased $[Ca^{2+}]_i$ 8.223±1.276 % compared with control group in the absence of extracellular calcium. Extracellular calcium (0.05 mM $CaCl_2$) enchanced the increase of $[Ca^{2+}]_i$ by TIP39 about 4.05 % (Figure 1b and 1c) compared with the absence of extracellular calcium (Figure 1c). Figure 1d and 1e show Ca^{2+} leakage from ER by stimulation of ionomycin in the absence of extracellular calcium. The peak of $[Ca^{2+}]_i$ increase from ER in control NHEK was 83.75 %, whereas 30min pretreatment of TIP39 was 39.15 % (Figure 1e). This data shows that TIP39 increased cytoplasmic Ca^{2+} from ER store in the absence of extracellular calcium. When extracellular calcium was added after TIP39 stimulation, ER Ca^{2+} store was rapidly refilled time in a time-dependent manner, a response likely aided by SERCA (supplementary Figure a). The depletion of ER Ca^{2+} by TIP39 (Figure 1e) was completely rescued by 2.5 mM $CaCl_2$ in 10min (Figure 1g). Those data suggest that TIP39 reduced ER Ca^{2+} store, but it immediately improved SERCA activity after supplementation of extracellular calcium.

The PTH2 receptor is expressed in the epidermis of Darier disease

Previous data suggests that TIP39 may enhance SERCA activity in certain conditions. We therefore hypothesized that TIP39 may have the potential to rescue some of the aspects of abnormal calcium transport and cell differentiation seen in DD skin. First, we obtained DD skin sections from Dr. Nakama at Kurume University (Kurume, Fukuoka, Japan), to evaluate the expression of PTH2R in these keratinocytes of patients with this disorder. Patient information is showed at Figure 2a. The patient has a mutation of E917 in L8-9 domain or R131 in A domain. The previous research showed R131 mutation reduced the expression of SERCA2b protein about 70% compared with wild type SERCA2b (16). E917 mutation was not tested, but S916 or S920 mutation reduced about 80% activity of Ca^{2+}-ATPase (16). Those results suggest that both patients' amino mutation induces severe SERCA2 dysfunction. The known histological features of DD including focal separation between suprabasal epidermal cells (acantholysis), suprabasal clefting and a distinctive dyskeratosis were seen in DD1 (Figure 2b middle). In DD2, widened epidermal cell-cell junction (spongeosis) was observed but acantholysis was not seen (Figure 2b right). PTH2R was detected sparsely in control epidermis as previously described, but both DD1 and DD2 epidermis expressed PTH2R abundantly throughout keratinocytes in the epidermis (Figure 2c, top and middle panels).

TIP39 has influence on cytosolic calcium in *ATP2A2* silenced-keratinocytes but the effect was incomplete

To establish an *in vitro* model of epidermal dysfunction as a consequence of decreased expression of ATP2A2, we transfected siRNA for *ATP2A2* to primary cultures of normal human epidermal keratinocytes (NHEK). Transfection of this siRNA succeeded in >90% gene knockdown and protein reduction of ATP2A2 as compared to siRNA control (Figure 3a, b). Other major paralogs of SERCA genes were not significantly changed by *ATP2A2* silencing (Figure 3a). Monolayer keratinocytes treated with siRNA to *ATP2A2* showed reduced desmoplakin expression (Figure 3c) as previously reported (5). To evaluate interactions between the SERCA2 activity and activation of PTH2R, the effects of TIP39 on *ATP2A2*-knockdown NHEK (ATP2A2 KD) were studied. TIP39 peptide was first added to NHEK grown in monolayer.

Figure 3d shows *ATP2A2* silencing effects on cytoplasmic calcium in NHEK. The basic Fluo-4 fluorescence has no significant difference between two groups (Figure 3d). For analyzing *ATP2A2* silencing effects on Ca^{2+} store in ER, ionomycin was used in the absence of extracellular calcium as in Figure 1d (Figure 3e). This data shows ER calcium content was not affected by *ATP2A2* silencing (Figure 3e). *ATP2A2* silencing delayed the Ca^{2+} efflux from ER to cytoplasm by TIP39 and accelerated the closure of the reaction (Figure 3f).

Figure 3g and 3h show imaging of the intracellular calcium probe Fluo-4 in NHEK at 5 minutes and 30 minutes after TIP39 or Thapsigargin treatment, respectively. 2mM $CaCl_2$ and 10μM ionomycin were used for positive controls. At 5 minutes post-stimulation, TIP39 increased intracellular calcium in both control and *ATP2A2*-silenced keratinocytes (Figure 3g). At 30min after stimulation, Fluo-4 accumulated at in the perinuclear region of TIP39

stimulated-NHEK, but it failed to accumulate after treatment with thapsigargin or *ATP2A2* knockdown (Figure 3h).

TIP39 improved intercellular clefts without keratinization in an *ATP2A2* silenced-3D epidermal model

Next, to evaluate the function of these cells when differentiated into a stratified model of human epidermis, NHEK were grown in 3D skin constructs on devitalized dermis (10). 300pmol siRNA was tranfected to undifferentiated monolayer NHEK 18 hours before being seeded into constructs (Supplementary figure b). Both gene and protein expression of ATP2A2 in 3D skin constructs were reduced in the construct transfected with target siRNA compared with its control (Figure 4a and 4b). Similar to the histological features of skin in DD, keratinocytes in this model of silenced *ATP2A2* displayed dyskeratosis (Figure 4c upper and middle panels), partial parakeratosis (Figure 4c upper and bottom panels), suprabasal clefts (Figure 4c middle panels) and abnormal cell-cell contact without reduction of E-cadherin (Figure 4c bottom panels). Epidermal hyperplasia, a thickened granular layer or hyperkeratosis were not seen. Having confirmed that DD epidermis expressed abundant PTH2R (Figure 2c), but also observing that TIP39 could not maintain $[Ca^{2+}]_i$ of *ATP2A2* KD after 30 minutes of stimulation (Figure 3h), it was necessary to evaluate the role of SERCA2 as a potential mediator of TIP39 action in *ATP2A2*-silenced skin constructs. Previously we reported that TIP39 induced terminal differentiation and increased stratum corneum thickness in the 3D skin construct (9). In this experiment, TIP39 also increased granular cell layer in control skin construct (data not shown), but it did not have this effect on keratinocyte differentiation of *ATP2A2*-silenced cells (Figure 4d right, 4e left and 4f). TIP39 reduced intercellular clefts of *ATP2A2*-silenced epidermis (Figure 4e right), and mRNA expression of desmoplakin (DSP) was not significantly changed by both *ATP2A2* silencing or TIP39 stimulation (Figure 4f).

Discussion

In this study, we report that TIP39 modulates ER calcium signaling and may have potential effects on Darier disease. TIP39 induced a shift of Ca^{2+} from the ER to the cytoplasm in the absence of extracellular calcium (Figure 1a and 1e), but the depletion of ER store was immediately rescued after supplementation with extracellular calcium (Figure 1g and Supplementary Figure a). This phenomenon suggests that TIP39 might increase SERCA activity by regulating ER calcium homeostasis. Attempts to use TIP39 to affect SERCA2 (ATP2A2) showed it increased cytosolic calcium in *ATP2A2* –silenced keratinocytes (Figure 3f and 3g), but the effects were incomplete compared with control (Figure 3f and 3h).

A 3D model of *ATP2A2* silenced keratinocyte showed histological features characteristic of DD including dyskeratosis, suprabasal clefts and parakeratosis, but did not show hyperplasia, thickened granular layer and remarkable hyperkeratosis. These results suggest that the pathophysiology of DD is likely not only due to a gene mutation of *ATP2A2* but may also be driven by other cell types that interact with these abnormal keratinocytes such as microbes, fibroblasts and/or immunocytes. Furthermore, we tested the capacity of TIP39 to enhance calcium transport in an attempt to rescue defects in calcium transport due to

mutations of *ATP2A2*. TIP39 reduced intercellular clefts in the DD-like epidermis, but did not induce keratinization. This intermediate effect was consistent with observations that TIP39 response was incomplete after silencing of *ATP2A2* (Figure 3f and 3h).

Vitamin D3 and the parathyroid hormone family member, PTHrP, can influence calcium homeostasis in keratinocytes, but the specific mechanisms of action on keratinocyte differentiation remain unclear. Topical vitamin D3 analogs are widely used for skin diseases such as psoriasis that manifest abnormalities of epidermal differentiation. The action of vitamin D3 on dyskeratosis is thought to involve calcium homeostasis and keratinocyte differentiation, but other factors such as immune responses are related to the disease severity and may influence clinical outcome. For example, topical vitamin D3 modulates development of immune cells and production of inflammatory cytokine in psoriasis skin (11, 17-19). This immune regulation may be due to a direct effect of calcium signaling on immune cell activation or differentiation such as mast cells, neutrophils, macrophages, dendritic and T cells (20-22).

DD often leads to secondary bacterial, fungal or viral infection of the skin. A limitation of the current study and model of DD is that these observations were made in a sterile environment, not in the physiological setting of active communication between resident skin microbes and the epidermis. Based on the phenotype observed in DD, it is likely that calcium signaling will either directly or indirectly influence host communication with bacteria by effects on immune cell function or epidermal penetration (20). In the future, it will be necessary to adapt the DD-like 3D epidermal model reported here to further investigate the function of microbes in the skin. However, the current study further illustrates the utility of TIP39 as a molecule to influence calcium homeostasis and the potential of 3D keratinocyte culture models to test therapies of genetic skin diseases.

Supplementary Material

Refer to Web version on PubMed Central for supplementary material.

Acknowledgements

The authors would like to thank all the members of the Gallo laboratory for the input and stimulating conversations.

This work was supported in part by NIH grants R01 AI116576, AR064781 and AI052453 (RLG) and the UCSD Dermatologist Investigator Training Program T32AR062496 (JAS, MRW).

References

1. Dhitavat J, Fairclough R J, Hovnanian A, et al. Calcium pumps and keratinocytes: lessons from Darier's disease and Hailey-Hailey disease. Br J Dermatol. 2004; 150:821–828. [PubMed: 15149492]
2. Ringpfeil F, Raus A, DiGiovanna J J, et al. Darier disease--novel mutations in ATP2A2 and genotype-phenotype correlation. Exp Dermatol. 2001; 10:19–27. [PubMed: 11168576]
3. Takagi A, Kamijo M, Ikeda S. Darier disease. J Dermatol. 2016; 43:275–279. [PubMed: 26945535]
4. Sakuntabhai A, Ruiz-Perez V, Carter S, et al. Mutations in ATP2A2, encoding a Ca2+ pump, cause Darier disease. Nat Genet. 1999; 21:271–277. [PubMed: 10080178]

5. Hobbs R P, Amargo E V, Somasundaram A, et al. The calcium ATPase SERCA2 regulates desmoplakin dynamics and intercellular adhesive strength through modulation of PKCα signaling. Faseb J. 2011; 25:990–1001. [PubMed: 21156808]

6. Savignac M, Simon M, Edir A, et al. SERCA2 dysfunction in Darier disease causes endoplasmic reticulum stress and impaired cell-to-cell adhesion strength: rescue by Miglustat. J Invest Dermatol. 2014; 134:1961–1970. [PubMed: 24390139]

7. Adase C A, Borkowski A W, Zhang L J, et al. Non-coding Double-stranded RNA and Antimicrobial Peptide LL-37 Induce Growth Factor Expression from Keratinocytes and Endothelial Cells. J Biol Chem. 2016; 291:11635–11646. [PubMed: 27048655]

8. Usdin T B, Hoare S R, Wang T, et al. TIP39: a new neuropeptide and PTH2-receptor agonist from hypothalamus. Nat Neurosci. 1999; 2:941–943. [PubMed: 10526330]

9. Sato E, Muto J, Zhang L J, et al. The parathyroid hormone second receptor PTH2R, and its ligand tuberoinfundibular peptide of 39 residues TIP39, regulate intracellular calcium and influence keratinocyte differentiation. J Invest Dermatol. 2016

10. Li J, Sen G L. Generation of Genetically Modified Organotypic Skin Cultures Using Devitalized Human Dermis. 2015:e53280.

11. Sato-Deguchi E, Imafuku S, Chou B, et al. Topical vitamin D(3) analogues induce thymic stromal lymphopoietin and cathelicidin in psoriatic skin lesions. Br J Dermatol. 2012; 167:77–84. [PubMed: 22384824]

12. Soboloff J, Rothberg B S, Madesh M, et al. STIM proteins: dynamic calcium signal transducers. Nat Rev Mol Cell Biol. 2012; 13:549–565. [PubMed: 22914293]

13. Meldolesi J, Pozzan T. The endoplasmic reticulum Ca2+ store: a view from the lumen. Trends Biochem Sci. 1998; 23:10–14. [PubMed: 9478128]

14. Berridge M J, Bootman M D, Roderick H L. Calcium signalling: dynamics, homeostasis and remodelling. Nat Rev Mol Cell Biol. 2003; 4:517–529. [PubMed: 12838335]

15. Mori M X, Itsuki K, Hase H, et al. Dynamics of receptor-operated Ca(2+) currents through TRPC channels controlled via the PI(4,5)P2-PLC signaling pathway. Front Pharmacol. 2015; 6:22. [PubMed: 25717302]

16. Miyauchi Y, Daiho T, Yamasaki K, et al. Comprehensive analysis of expression and function of 51 sarco(endo)plasmic reticulum Ca2+-ATPase mutants associated with Darier disease. J Biol Chem. 2006; 281:22882–22895. [PubMed: 16766529]

17. Kiso H, Ohba T, Iino K, et al. Sildenafil prevents the up-regulation of transient receptor potential canonical channels in the development of cardiomyocyte hypertrophy. Biochem Biophys Res Commun. 2013; 436:514–518. [PubMed: 23764398]

18. Pani B, Cornatzer E, Cornatzer W, et al. Up-regulation of transient receptor potential canonical 1 (TRPC1) following sarco(endo)plasmic reticulum Ca2+ ATPase 2 gene silencing promotes cell survival: a potential role for TRPC1 in Darier's disease. Mol Biol Cell. 2006; 17:4446–4458. [PubMed: 16899508]

19. Muehleisen B, Gallo R L. Vitamin D in allergic disease: shedding light on a complex problem. The Journal of allergy and clinical immunology. 2013; 131:324–329. [PubMed: 23374263]

20. Lee P H, Trowbridge J M, Taylor K R, et al. Dermatan sulfate proteoglycan and glycosaminoglycan synthesis is induced in fibroblasts by transfer to a three-dimensional extracellular environment. J Biol Chem. 2004; 279:48640–48646. [PubMed: 15347686]

21. Borkowski A W, Park K, Uchida Y, et al. Activation of TLR3 in keratinocytes increases expression of genes involved in formation of the epidermis, lipid accumulation, and epidermal organelles. J Invest Dermatol. 2013; 133:2031–2040. [PubMed: 23353987]

22. Simpson C L, Kojima S, Getsios S. RNA interference in keratinocytes and an organotypic model of human epidermis. Methods Mol Biol. 2010; 585:127–146. [PubMed: 19908001]

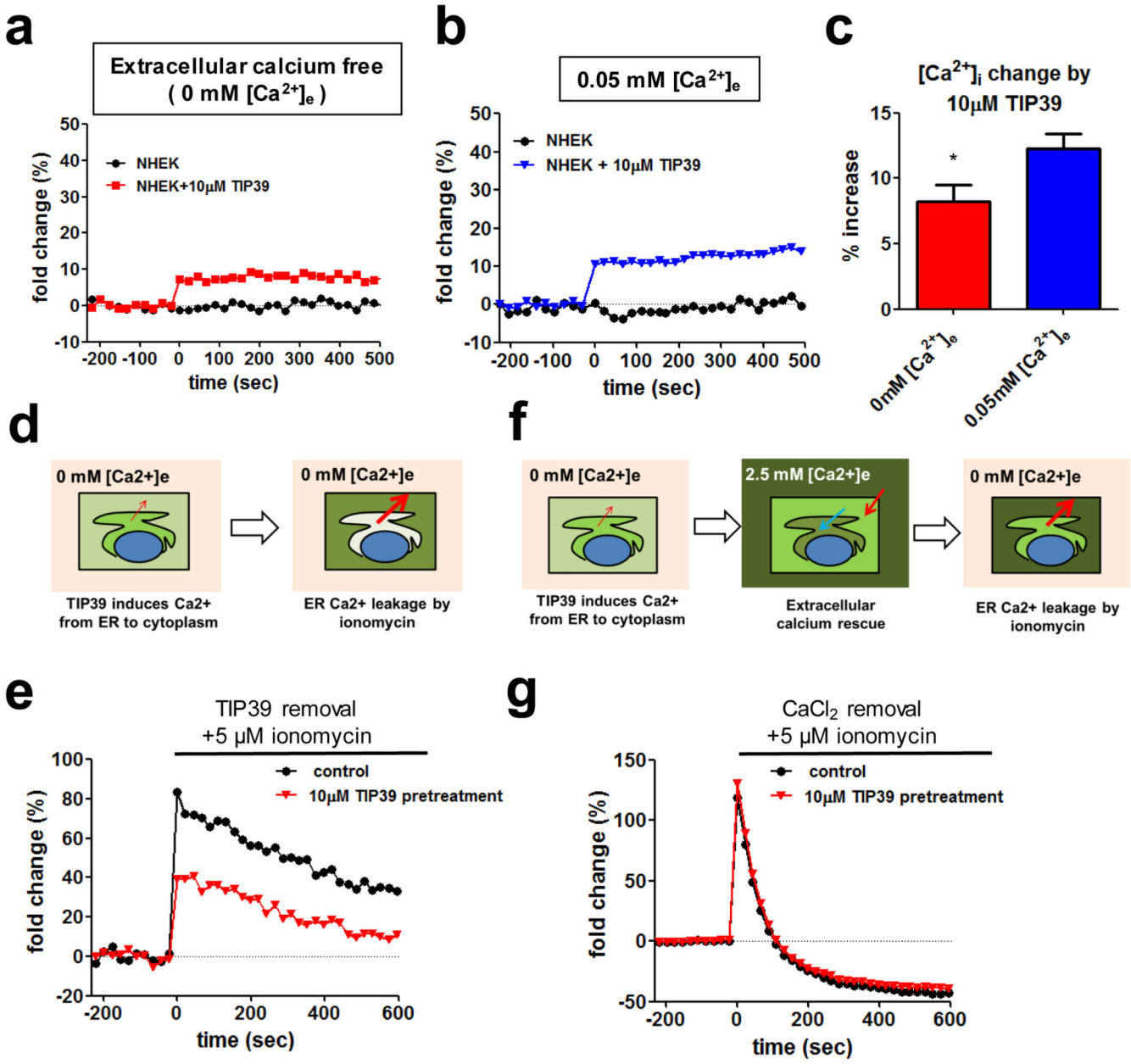

Figure 1. TIP39 increased intracellular calcium from ER and enhanced SERCA activity after extracellular Ca^{2+} supplementation

(a) Intracellular calcium change by 10μM TIP39 was monitored in the absence of extracellular calcium or **(b)** low calcium (0.05mM $CaCl_2$) contained-balanced salt solution. Both (a) and (b) samples were incubated for 70min in those salt solution before monitoring. For complete removal of extracellular calcium, 150 μM EGTA was added in the calcium-free solution of (a). **(c)** The bar graph shows comparison of % $[Ca^{2+}]$i increase of (a) and (b). The data were randomly extracted at 5 time points in 10 min after TIP39 stimulation. (Each group n=5, total n=25) **(d)** An experimental schema of (e), which analyzes ER Ca^{2+} content after TIP39 pretreatment. **(e)** ER Ca^{2+} content was monitored after 5 μM ionomycin stimulation with or without 30min pretreatment of 10μM TIP39 in the absence of

extracellular calcium. **(f)** An experimental schema of (g), which analyzes ER Ca^{2+} content after extracellular calcium rescue. **(g)** ER Ca^{2+} content was monitored after stimulation of 5 μM ionomycin with 10min rescue of 2.5 mM $CaCl_2$. Fold change (%) = (F-F0) / F0×100, F0 was the baseline calculated by averaging five time points just prior to the application of the stimulus. Data are means ± SEM, n=5 and are representative data from two independent experiments.*p<0.05 (Student's *t*-test).

a

	race	age	sex	biopsy	gene mutation	Amino mutation
Healthy control	asian	33	female	trunk	n/a	
Darier disease1	asian	57	male	trunk	*ATP2A2:* G⇒A at c.2749 in exon 19	Glu917Lys
Darier disease 2	asian	11	female	trunk	*ATP2A2:* G⇒A at c.392 in exon 5	Arg131Glu

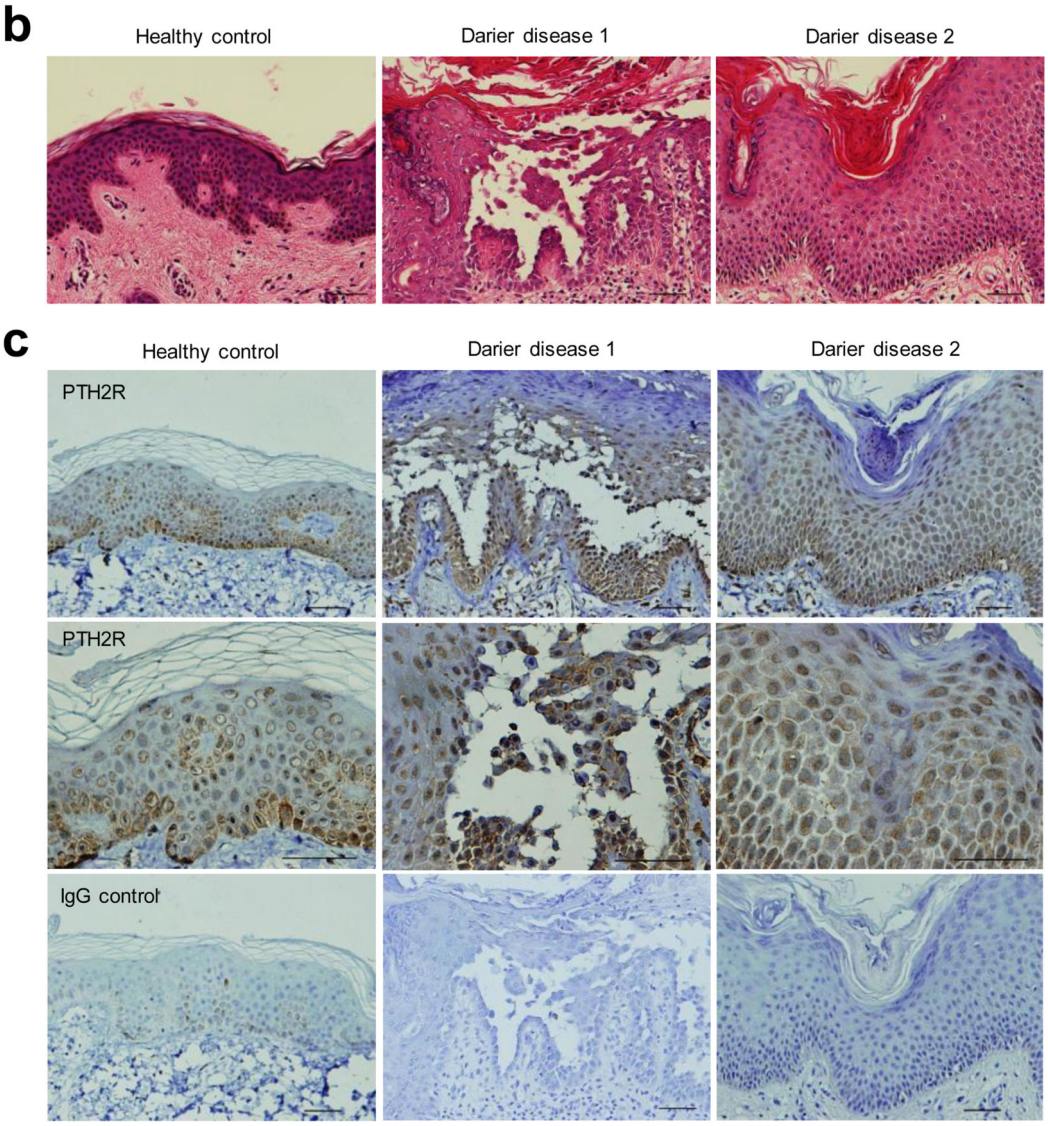

Figure 2. PTH2R is expressed in the epidermis of Darier disease

(a) Patient demographics and site of *ATP2A2* mutation are shown. **(b)** H&E staining and **(c)** immunohistochemistry of PTH2R (top and middle) of patients' skin sections. Rabbit IgG controls are bottom panels. Scale bars, 50μm.

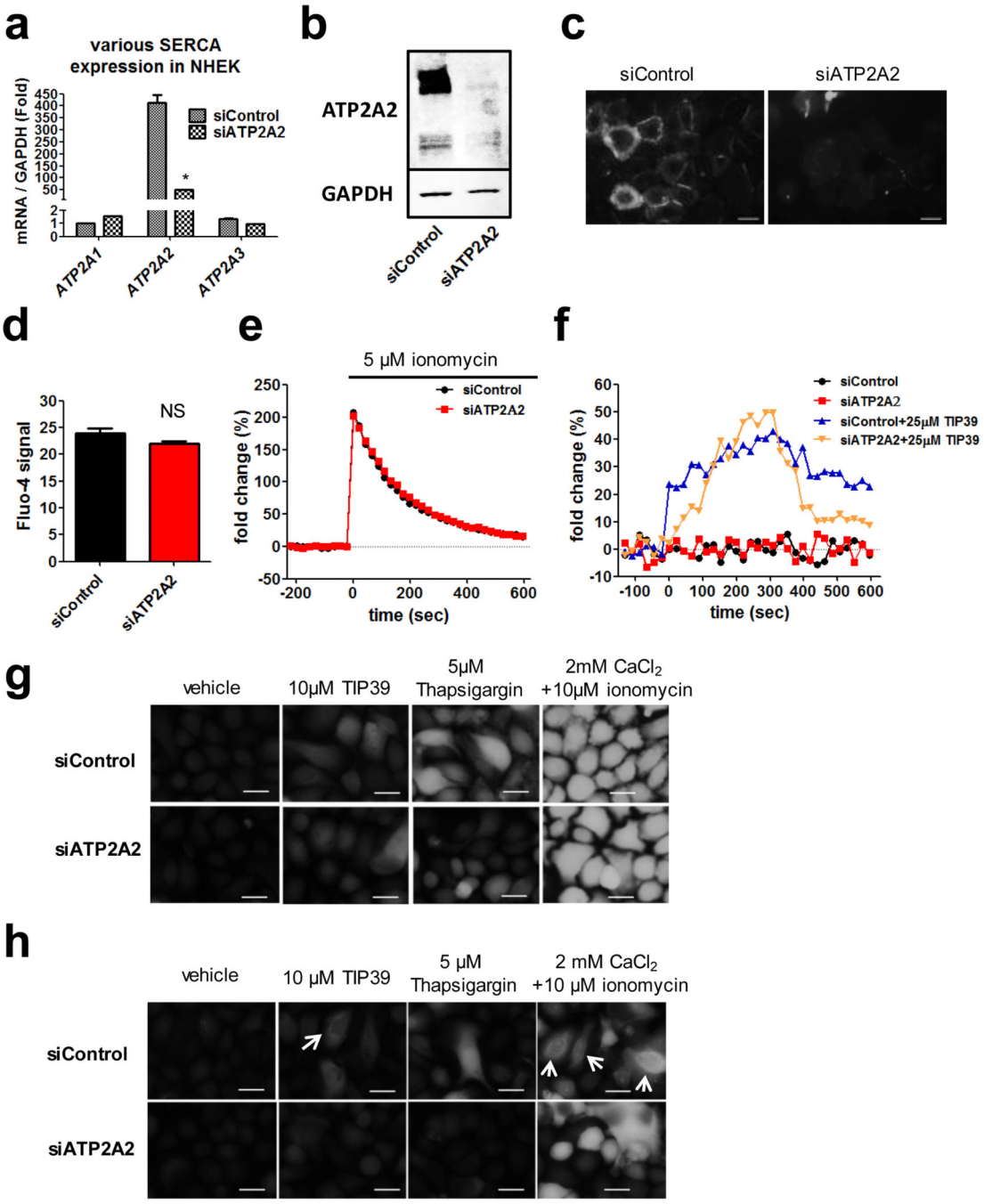

Figure 3. TIP39 increased cytosolic calcium in *ATP2A2* silenced-keratinocyte, but the reaction was incomplete compared with control

(a) NHEK were transfected siRNA for 72h then analyzed by qRT-PCR and **(b)** western blotting of ATP2A2 and GAPDH. GAPDH is used for housekeeping gene and protein. **(c)** Immunofluorescence staining of desmoplakin in siRNA transfected NHEK. Scale bars, 20μm. **(d)** Basic fluo-4 signal of siRNA transfected-NHEK in the absence of extracellular calcium. **(e)** ER calcium content was monitored after 5μM ionomycin stimulation in the absence of extracellular calcium. **(f)** Cytoplasmic calcium was monitored after stimulation of

25μM TIP39 in the absence of extracellular calcium. **(g)** Intracellular calcium imaging of siRNA transfected-keratinocytes. Cells were treated by 10μM TIP39, 5μM thapsigargin or 2mM $CaCl_2$ and 10μM ionomycin, then checked by microscopy at 5min and **(h)** 30min after stimulation. Scale bars, 20μm. Fold change (%) = (F-F0) / F0×100, Data are means ± SEM of biological replicates, n=3 (qRT-PCR) or n=5 (calcium assay) and are representative data from at least two independent experiments. .*$p<0.05$ (Student's *t*-test).

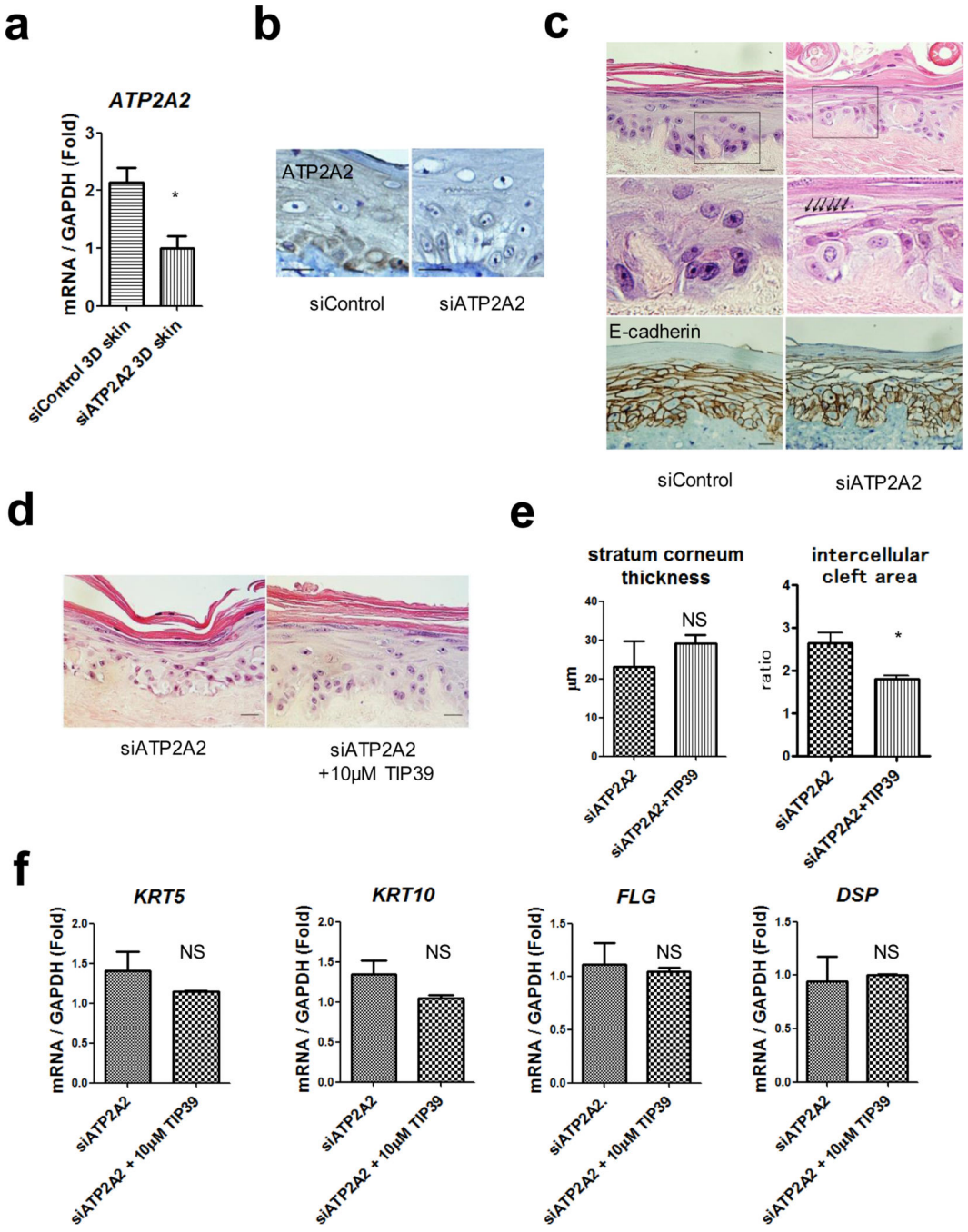

Figure 4. ***ATP2A2*** **silenced- 3D cultured keratinocyte model displayed dyskeratosis, partial parakeratosis and suprabasal clefts. TIP39 improved intercellular cleft area without hyperkeratosis**

NHEK were transfected with siRNA for *ATP2A2*, then used for development of a 3D model of DD by applying cells to devitalized human dermis. **(a)** Silencing effects of *ATP2A2* were analyzed by qRT-PCR and **(b)** immunohistochemical staining (IHC). H&E (top and middle panels) and IHC of E-cadherin (bottom panels) were shown at **(c)**. **(d)** H&E staining of siRNA transfected- in vitro 3D skin constructs. 3D skin constructs were then cultured with 10μM TIP39. Scale bars, 20μm. **(e)** Stratum corneum thickness or the area of intercellular

clefts were calculated by Image J. Data are means ± SEM, n=25 (total 2mm^2 analysis area). *p<0.05 (Student's *t*-test). **(f)** mRNA expression of indicated genes in the 3D skin constructs as determined by qPCR (*KRT5*= Keratin 5, *KRT10*=Keratin 10, *FLG*=Fillagrin, *DSP*=Desmoplakin). qRT-PCR data are means ± SEM of technical replicates from n=3. *p* values were calculated by student's*t*-test.*p<0.05 .